PROCEEDINGS OF SCIENCE

Combining low- and high-energy constraints on flavourful EFTs

Lukas Allwicher,[a,*] **Darius A. Faroughy,**[b] **Florentin Jaffredo,**[c] **Olcyr Sumensari**[d] **and Felix Wilsch**[a]

[a] *Physik-Institut, Universität Zürich,*
Winterthurerstrasse 190, 8057 Zurich, Switzerland
[b] *Department of Physics and Astronomy, Rutgers University,*
Piscataway, NJ 08854, USA
[c] *INFN - Sezione di Pisa,*
Largo Bruno Pontecorvo, 3/Edificio C, 56127 Pisa PI, Italy
[d] *IJCLab,*
Pôle Théorie (Bat. 210), CNRS/IN2P3 et Université, Paris-Saclay, 91405 Orsay, France
E-mail: lukas.allwicher@physik.uzh.ch, darius.faroughy@rutgers.edu, florentin.jaffredo@pi.infn.it, olcyr.sumensari@ijclab.in2p3.fr, felix.wilsch@physik.uzh.ch

The study of high-p_T tails at the LHC can be a complementary probe to low-energy observables when investigating the flavour structure of the Standard Model and its extensions. Motivated by the B anomalies, we study the interplay between low-energy observables, and both charged and neutral current Drell-Yan measurements. The `Mathematica` package `HighPT` allows to do so within a unified and consistent framework, yielding a likelihood function that includes not only high-p_T and flavor observables, but the EW pole and Higgs observables as well, thus allowing to perform combined fits easily. We discuss such combined analyses within the Effective Field Theory approach.

41st International Conference on High Energy physics - ICHEP2022
6-13 July, 2022
Bologna, Italy

*Speaker

© Copyright owned by the author(s) under the terms of the Creative Commons Attribution-NonCommercial-NoDerivatives 4.0 International License (CC BY-NC-ND 4.0).

PoS(ICHEP2022)753

1. Introduction

Solutions of long-standing problems in the Standard Model (SM), such as the hierarchy, point to New Physics (NP) at the TeV-scale. Moreover, there are motivated approaches to the flavour puzzle, based on multi-scale scenarios, in which the lowest NP scale lies in the same range (see e.g. [2]). The flavour structure of generic NP scenarios, however, is tightly constrained by flavour-physics, with the strongest bound on the scale coming from the kaon sector ($\Lambda_{\rm NP} \gtrsim 10^5$ TeV). This implies that some flavour assumptions (e.g. MFV [1], $U(2)^5$ [3]) need to be made on the NP in order to lower the bound down to the TeV-scale. With hypothetical NP at a few TeV, it is natural to consider the LHC as a complementary probe with respect to low-energy experiments and electroweak precision tests. Guided by the recent interest in semileptonic transitions, we focus, from the high-p_T side, on Drell-Yan measurements, and provide an example of how high-energy and low-energy measurements can be complementary in constraining the same NP scenarios. The results are derived using the `Mathematica` package `HighPT` [4, 5],

2. EFT setup: connecting observables at different energy scales

Under the assumption of heavy NP, the best way of parametrising effects at low energies, such as the EW scale or the B meson mass, is through an Effective Field Theory (EFT) approach. Above the EW scale, we can use the so-called Standard Model Effective Field Theory (SMEFT) [6, 7]. This is the theory obtained by complementing the SM lagrangian with higher-dimensional operators, constructed out of all SM fields, and invariant under $SU(3)_c \times SU(2)_L \times U(1)_Y$ gauge symmetry:

$$\mathcal{L}_{\rm SMEFT} = \mathcal{L}_{\rm SM} + \sum_{\alpha, d>4} \frac{C_\alpha}{\Lambda^{d-4}} O_\alpha^{(d)} \,. \tag{1}$$

In the broken phase of the SM, i.e. at energies below ~ 200 GeV, the SMEFT gets replaced by the Low-Energy Effective Theory (LEFT), invariant under $SU(3)_c \times U(1)_{\rm em}$, and with the heavy SM fields (H, t, $W^\pm$ and Z) integrated out. When evaluating the theory prediction for an observable, the matrix elements and Wilson coefficients need to be evaluated at the relevant energy scale, meaning that Renormalization Group Equation (RGE) running effects have to be taken into account when going from $\Lambda_{\rm NP}$, at which the SMEFT coefficients are generated, to e.g. $\mu_{\rm ew}$ or m_b. In the latter case, the full chain of SMEFT running, SMEFT-LEFT matching and LEFT running needs to be evaluated in order to get the LEFT coefficients at the B-physics scale. As a simple example, consider the semileptonic operator (in the SMEFT)

$$[O_{lq}^{(3)}]_{\alpha\beta ij} = (\bar{l}_\alpha \gamma_\mu \sigma^I l_\beta)(\bar{q}_i \gamma^\mu \sigma^I q_j) \,. \tag{2}$$

From [8] we know that

$$[\dot{C}_{Hl}^{(3)}]_{\alpha\beta} \supset 2N_c [C_{lq}^{(3)}]_{\alpha\beta kl} [Y_d^\dagger Y_d + Y_u^\dagger Y_u]_{lk} \,, \qquad [O_{Hl}^{(3)}]_{\alpha\beta} = (H^\dagger i D_\mu \sigma^I H)(\bar{l}_\alpha \gamma^\mu \sigma^I l_\beta) \,, \tag{3}$$

gives by solving the RGE with a leading-log approximation

$$[C_{Hl}^{(3)}]_{\alpha\beta}(\mu_{\rm ew}) = 2N_c [C_{lq}^{(3)}]_{\alpha\beta kl} [Y_d^\dagger Y_d + Y_u^\dagger Y_u]_{lk} \log \frac{\mu_{\rm ew}}{\Lambda_{\rm NP}} \,. \tag{4}$$

PoS(ICHEP2022)753

The operator above yields a modification of the W boson couplings to leptons:

$$\mathcal{L}_{\text{eff}}^{W} = -\frac{g}{\sqrt{2}} \sum_{\alpha,\beta} \left[g_{\ell_L}^{W\,\alpha\beta} \left(\bar{\ell}_{L\alpha} \gamma^{\mu} \nu_{L\beta} \right) \right] W_{\mu} + \text{h.c.} \tag{5}$$

$$g_{\ell_L}^{W\,\alpha\beta} = \delta_{\alpha\beta} + \frac{v^2}{\Lambda^2} [C_{Hl}^{(3)}]_{\alpha\beta} \tag{6}$$

This shows how a four-fermion operator, originating from some UV dynamics, can have an effect in EW precision observables [9].

3. Input parameters and input redefinitions

When searching for NP effects, it is important to be clear about the experimental inputs used to determine the SM predictions for the different observables, and how these may be affected by NP, in order to avoid inconsistencies. Indeed, a NP contribution to an observable used to extract e.g. one of the gauge parameters of the SM is technically not observable, it will however affect all other observables in which said parameter appears. For example, the Fermi constant G_F, extracted from μ decays, will enter all weak interaction processes. Parametrising the NP contributions to the μ decay in SMEFT, and defining $G_F = G_F^{(0)} + \delta G_F$, where $G_F^{(0)}$ is the "bare" SM value, one finds

$$\frac{\delta G_F}{G_F^{(0)}} = \frac{v^2}{\Lambda^2} \left(\left[C_{Hl}^{(3)}\right]_{22} + \left[C_{Hl}^{(3)}\right]_{11} - \frac{1}{2}\left[C_{ll}\right]_{2112} - \frac{1}{2}\left[C_{ll}\right]_{1221} \right) + O\left(\frac{v^4}{\Lambda^4}\right). \tag{7}$$

Not only the gauge parameters are affected by this, but also the extraction of the CKM elements. Extracting the matrix elements from semileptonic meson decays, NP contributions can be parametrised as [10]

$$\frac{\mathcal{B}(P \to P' \ell \bar{\nu})}{\mathcal{B}(P \to P' \ell \bar{\nu})^{\text{SM}}} = \frac{|V_{ij}|^2}{|V_{ij}^{(0)}|^2} = \sum_{\alpha\beta} \rho_{\alpha\beta}^{ij\,\ell}(\mu)\, C_{\alpha}^{ij\,\ell}(\mu)\, C_{\beta}^{ij\,\ell}(\mu)^{*}, \tag{8}$$

where $\rho_{\alpha\beta}$ are numerical coefficients computed using hadronic form-factors, and C_α are LEFT Wilson coefficients. Defining again $|V_{ij}| = |V_{ij}^{(0)}| + \delta|V_{ij}|$, we find that, for example,

$$|V_{ud}^{(0)}| = 1 - \frac{V_{us}^2}{2} - \frac{V_{us}^4}{8} + \delta|V_{us}| \left(V_{us} + \frac{V_{us}^3}{2} \right) + O(\delta|V_{us}|^2), \tag{9}$$

where $\delta|V_{us}|$ is a function of the Wilson coefficients that can be extracted from Eq. (8) with the appropriate choice of quark flavour indices.

Our input scheme is $\{G_F, m_Z, \alpha_{\text{em}}, \alpha_S\}$ for the gauge parameters, with numerical values as in [11]. All other quantities can be expressed as a function of these, plus the Higgs and top-quark masses. For example,

$$\cos^2\theta_W = \frac{1}{2}\left[1 + \left(1 - \frac{4\pi\alpha_{\text{em}}}{\sqrt{2} G_F m_Z^2} \right)^{1/2} \right]. \tag{10}$$

The CKM matrix elements are determined as follows:

PoS(ICHEP2022)753

- $|V_{us}|$: from the PDG average of $\mathcal{B}(K^+ \to \pi^0 e^+ \nu)$ and $\mathcal{B}(K_L \to \pi^\pm e^\mp \nu)$ [12].
- $|V_{cb}|$: from the HFLAV average of $\mathcal{B}(B^0 \to D^- \ell^+ \nu)$ and $\mathcal{B}(B^+ \to D^0 \ell^+ \nu)$, with $\ell = e, \mu$ [13].
- $|V_{ub}|$: from the BaBar and Belle determinations $\dfrac{\mathrm{d}\Gamma(B \to \pi \ell \bar{\nu})}{\mathrm{d}q^2}$ at high-q^2 ($q^2 > 16$ GeV^2 bin) [14, 15].
- γ: from the UTfit NP analysis [16].

With these inputs, our CKM matrix reads

$$V = \begin{pmatrix} 0.97487(15) & 0.2228(6) & 0.0039(2)\, e^{-i\,68.7(4.2)^\circ} \\ -0.2231(7) & 0.9739(7) & 0.0405(4) \\ 0.0084(3)\, e^{-i\,24.8(1.4)^\circ} & -0.0398(4)\, e^{i\,1.13(7)^\circ} & 0.998990(11) \end{pmatrix}. \tag{11}$$

4. An example using `HighPT`: LFU tests in $b \to c\ell\nu$ transitions

As an illustration, we show how high-p_T Drell-Yan searches combine with other measurements in the case of LFU tests in charged current B-decays. The observables of interest at low-energy are

$$R_{D^{(*)}} = \left.\frac{\mathcal{B}(B \to D^{(*)}\tau\nu)}{\mathcal{B}(B \to D^{(*)}\ell\nu)}\right|_{\ell \in \{e\,\mu\}}, \tag{12}$$

which have recently been updated with a new measurement from LHCb [17] and are still showing a tension with the SM. The low-energy description goes through the effective lagrangian

$$\mathcal{L}_{\text{eff}}^{b\to c\tau\nu} = -2\sqrt{2} G_F V_{cb} \Big[(1 + C_{V_L}) (\bar{c}_L \gamma_\mu b_L)(\bar{\tau}_L \gamma_\mu \nu_L) + C_{V_R} (\bar{c}_R \gamma_\mu b_R)(\bar{\tau}_L \gamma_\mu \nu_L) \tag{13}$$

$$+ C_{S_L} (\bar{c}_R b_L)(\bar{\tau}_R \nu_L) + C_{S_R} (\bar{c}_L b_R)(\bar{\tau}_R \nu_L) + C_T (\bar{c}_R \sigma_{\mu\nu} b_L)(\bar{\tau}_R \sigma^{\mu\nu} \nu_L) \Big] + \text{h.c.}\,. \tag{14}$$

There are three viable leptoquark scenarios to explain the anomaly (see [18]): (i) the vector $U_1 \sim (\mathbf{3}, \mathbf{1}, 2/3)$, and the scalars (ii) $S_1 \sim (\bar{\mathbf{3}}, \mathbf{1}, 1/3)$ and (iii) $R_2 \sim (\mathbf{3}, \mathbf{2}, 7/6)$. The most relevant operators, at the matching scale Λ for each of these scenarios are [1]

$$U_1 : \left[C_{lq}^{(1)}\right]_{3323} = \left[C_{lq}^{(3)}\right]_{3323}, \qquad \left[C_{lq}^{(1)}\right]_{3333} = \left[C_{lq}^{(3)}\right]_{3333}, \qquad \left[C_{ledq}\right]_{3333}. \tag{15}$$

$$S_1 : \left[C_{lq}^{(1)}\right]_{3333} = -\left[C_{lq}^{(3)}\right]_{3333}, \qquad \left[C_{lequ}^{(1)}\right]_{3332} = -4 \left[C_{lequ}^{(3)}\right]_{3332}. \tag{16}$$

$$R_2 : \left[C_{lequ}^{(1)}\right]_{3332} = 4 \left[C_{lequ}^{(3)}\right]_{3332}. \tag{17}$$

At high-p_T, the relevant processes are

$$pp \to \tau\tau, \qquad pp \to \tau\nu, \tag{18}$$

[1] The coefficients refer to operators expressed in the Warsaw basis [7]

PoS(ICHEP2022)753

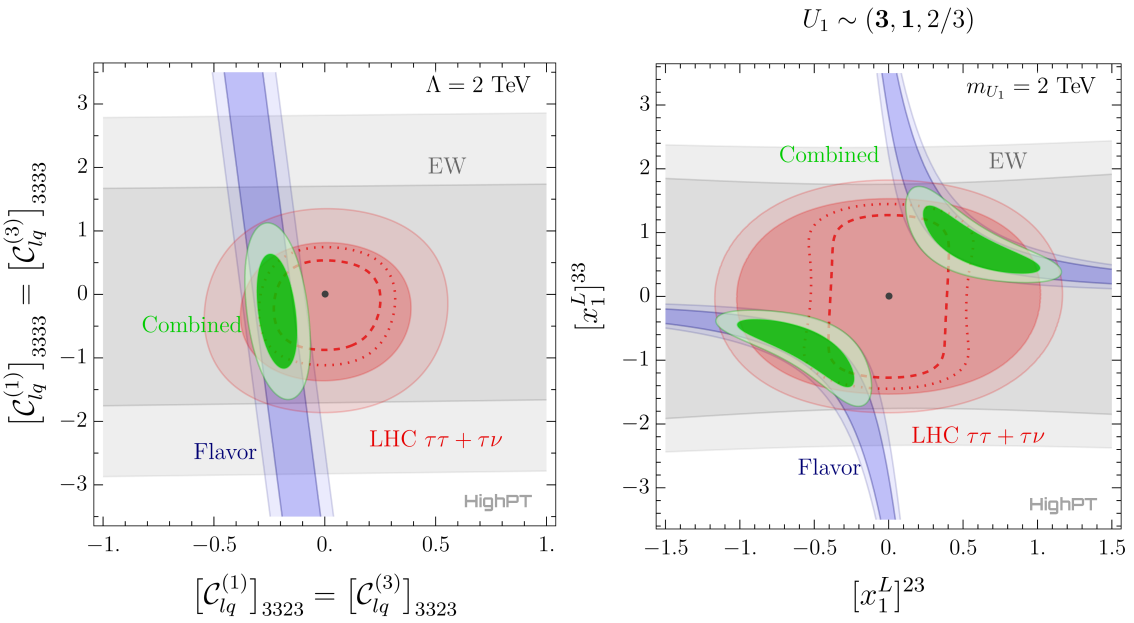

Figure 1: 1σ and 2σ preferred regions for $R_{D^{(*)}}$ (blue), EW observables (gray), $pp \to \tau\tau(\tau\nu)$ (red), and their combination (green). The dashed (dotted) red lines indicate 1σ and 2σ projections for the high-luminosity phase of LHC (3 ab^{-1}).

and their likelihoods can be computed within `HighPT` (for more details on the package see [4, 5] and the talk by Florentin Jaffredo at this conference). In Figure 1 we show the results of the fit, including also EW observables, for the U_1 case. On the left panel, the LHC likelihood has been computed in the SMEFT, i.e. not including possible propagation effects of the leptoquark. On the right, such effects are accounted for, and the likelihood is computed directly in terms of the U_1 couplings to fermions, which are governed by the lagrangian

$$\mathcal{L}_{U_1} = [x_1^L]_{i\alpha}\, \bar{q}_i \not{U}_1 l_\alpha + [x_1^R]_{i\alpha}\, \bar{d}_i \not{U}_1 e_\alpha + \text{h.c.} \tag{19}$$

and we chose to switch on only $[x_1^L]_{23,33}$, since these are the couplings needed to generate the operators in Eq. (15). It is worth noticing, however, that also the operators $[C_{lq}^{(1,3)}]_{3322}$ are generated in this case, giving for example additional contributions to the $pp \to \tau\tau$ cross-section. From the plots one can see that the information coming from LHC is already restricting the viable parameter space, with room for improvement coming from the high-luminosity phase of LHC.

5. Summary and outlook

High-p_T tails measured at LHC can give complementary and competitive constraints on NP compared to low-energy experiments. The package `HighPT` provides an easy-to-use framework to extract LHC likelihoods from Run-2 ATLAS and CMS Drell-Yan searches, with all possible leptonic final states. In a future release, the ideas and methodology presented in this proceeding will be included in the package, allowing for a combined analysis of high- and low-energy observables, within a unified and well-defined framework.

PoS(ICHEP2022)753

References

[1] G. D'Ambrosio, G. F. Giudice, G. Isidori and A. Strumia, Nucl. Phys. B **645** (2002), 155-187 doi:10.1016/S0550-3213(02)00836-2 [arXiv:hep-ph/0207036 [hep-ph]].

[2] M. Bordone, C. Cornella, J. Fuentes-Martin and G. Isidori, Phys. Lett. B **779** (2018), 317-323 doi:10.1016/j.physletb.2018.02.011 [arXiv:1712.01368 [hep-ph]].

[3] R. Barbieri, G. Isidori, J. Jones-Perez, P. Lodone and D. M. Straub, Eur. Phys. J. C **71** (2011), 1725 doi:10.1140/epjc/s10052-011-1725-z [arXiv:1105.2296 [hep-ph]].

[4] L. Allwicher, D. A. Faroughy, F. Jaffredo, O. Sumensari and F. Wilsch, [arXiv:2207.10714 [hep-ph]].

[5] L. Allwicher, D. A. Faroughy, F. Jaffredo, O. Sumensari and F. Wilsch, [arXiv:2207.10756 [hep-ph]].

[6] W. Buchmuller and D. Wyler, Nucl. Phys. B **268** (1986), 621-653 doi:10.1016/0550-3213(86)90262-2

[7] B. Grzadkowski, M. Iskrzynski, M. Misiak and J. Rosiek, JHEP **10** (2010), 085 doi:10.1007/JHEP10(2010)085 [arXiv:1008.4884 [hep-ph]].

[8] E. E. Jenkins, A. V. Manohar and M. Trott, JHEP **01** (2014), 035 doi:10.1007/JHEP01(2014)035 [arXiv:1310.4838 [hep-ph]].

[9] F. Feruglio, P. Paradisi and A. Pattori, JHEP **09** (2017), 061 doi:10.1007/JHEP09(2017)061 [arXiv:1705.00929 [hep-ph]].

[10] S. Descotes-Genon, A. Falkowski, M. Fedele, M. González-Alonso and J. Virto, JHEP **05** (2019), 172 doi:10.1007/JHEP05(2019)172 [arXiv:1812.08163 [hep-ph]].

[11] A. Falkowski and D. Straub, JHEP **04** (2020), 066 doi:10.1007/JHEP04(2020)066 [arXiv:1911.07866 [hep-ph]].

[12] P. A. Zyla *et al.* [Particle Data Group], PTEP **2020**, no.8, 083C01 (2020) doi:10.1093/ptep/ptaa104

[13] Y. S. Amhis *et al.* [HFLAV], Eur. Phys. J. C **81**, no.3, 226 (2021) doi:10.1140/epjc/s10052-020-8156-7 [arXiv:1909.12524 [hep-ex]].

[14] J. P. Lees *et al.* [BaBar], Phys. Rev. D **86**, 092004 (2012) doi:10.1103/PhysRevD.86.092004 [arXiv:1208.1253 [hep-ex]].

[15] A. Sibidanov *et al.* [Belle], Phys. Rev. D **88**, no.3, 032005 (2013) doi:10.1103/PhysRevD.88.032005 [arXiv:1306.2781 [hep-ex]].

[16] M. Bona *et al.* [UTfit], JHEP **03**, 049 (2008) doi:10.1088/1126-6708/2008/03/049 [arXiv:0707.0636 [hep-ph]].

PoS(ICHEP2022)753

[17] G. M. Ciezarek (LHCb), CERN Seminar, https://indico.cern.ch/event/1187939/

[18] A. Angelescu, D. Bečirević, D. A. Faroughy, F. Jaffredo and O. Sumensari, Phys. Rev. D **104** (2021) no.5, 055017 doi:10.1103/PhysRevD.104.055017 [arXiv:2103.12504 [hep-ph]].

PoS(ICHEP2022)753